

Quasi-one-dimensional soliton in a self-repulsive spin-orbit-coupled dipolar spin-half and spin-one condensates

S. K. Adhikari*

Instituto de Física Teórica, Universidade Estadual Paulista - UNESP, 01.140-070 São Paulo, São Paulo, Brazil

(Dated: March 2, 2026)

We study the formation of solitons in a uniform quasi-one-dimensional (quasi-1D) spin-orbit (SO) coupled self-repulsive pseudo spin-half and spin-one dipolar Bose-Einstein condensates (BEC), using the mean-field Gross-Pitaevskii equation. The dipolar atoms are taken to be polarized along the quasi-1D x direction. In the pseudo spin-half case, for small SO-coupling, one can have dark-bright and bright-bright solitons. For large SO coupling, the dark-bright and bright-bright solitons may acquire a spatially-periodic modulation in density; for certain values of contact interaction parameters there is only the normal bright-bright soliton without any spatially-periodic modulation in density. In the spin-one anti-ferromagnetic case, for small SO coupling, one can have bright-bright-bright, dark-bright-dark, and bright-dark-bright solitons; and for large SO coupling, the dark-bright-dark and bright-dark-bright solitons are found to have a spatially-periodic modulation in density. In the spin-one ferromagnetic case, for both small and large SO coupling, we find only bright-bright-bright solitons. All these solitons, specially those with a dark-soliton component, are dynamically stable as demonstrated by real-time propagation using the converged stationary solution obtained by imaginary-time propagation as the initial state.

I. INTRODUCTION

A bright soliton is a one-dimensional (1D) self-bound localized strongly-stable solitary wave that travel with a constant velocity maintaining its shape due to a cancellation of linear repulsion and nonlinear attraction. Such solitons have been found in a nonlinear medium [1], in water waves, in nonlinear optics [2], and in a Bose-Einstein condensate [3] (BEC) among others. Quasi-1D bright solitons have been created in a BEC of ^7Li [4, 5] and ^{85}Rb [6] atoms, by a management of the nonlinear attraction near a Feshbach resonance [7], following the suggestion of a theoretical investigation [8], using the mean-field Gross-Pitaevskii (GP) equation [9, 10]. There have been many studies of quasi-1D solitons in a BEC [11–17]. Dark solitons were also observed and studied in nonlinear optical fibers [18–20] and in a BEC of ^{87}Rb atoms [21, 22]. A general dark soliton can also travel freely and is an envelope soliton having the form of a density dip with a phase jump across its density minimum [23]. Bright (dark) solitons have a maximum (minimum) of density at the center. Although, the bright solitons in a BEC have a long lifetime, the dark solitons have a short lifetime and are usually unstable not only in a BEC [21, 24, 25] but also in a general nonlinear system [26].

Not long after the observation [27] of condensates of ^{85}Rb , ^{87}Rb , ^7Li and ^{23}Na atoms in a laboratory, Stenger et al. observed and studied a hyper-fine spin-one three-component spinor BEC of ^{23}Na atoms [28]. There cannot be a usual spin-orbit (SO) coupling between two electrically neutral atoms in a BEC. The next step forward was the successful creation of an artificial synthetic SO cou-

pling by tuning a few Raman laser beams which couple two [29] or three [30] hyper-fine spin states of electrically neutral spin-one ^{87}Rb [31–33] and ^{23}Na [34] atoms, thus generating an SO-coupled pseudo spin-half or a spin-one BEC. Multi-component SO-coupled spinor BECs possess distinct properties and can have different excitations [35, 36], which are not allowed in a single-component scalar BEC. For example, a quasi-1D [37] soliton stabilized in a pseudo spin-half or a spin-one SO-coupled BEC can have distinct spatial structure [38, 39].

The long-range non-local dipolar interaction allows the formation of different types of quasi-1D solitons in a BEC, which is not possible in the absence of a dipolar interaction. After the experimental observation of dipolar BECs of ^{52}Cr [40–42], ^{166}Er [43], ^{168}Er [44], and ^{164}Dy [45, 46] atoms, with a large magnetic dipole moment, we find it highly relevant to perform a detailed study of quasi-1D solitons in an SO-coupled pseudo spin-half and spin-one dipolar BEC. There have been a few previous studies on different aspects of an SO-coupled dipolar BEC [47–57] as well as on the formation of a quasi-1D [38, 58–60], quasi-two-dimensional (quasi-2D) [61, 62] and quasi-three-dimensional [63] soliton in an SO-coupled nondipolar BEC. These previous studies on SO-coupled nondipolar BEC solitons were performed on a *self-attractive* BEC with negative intraspecies and interspecies scattering lengths, where solitons are possible even in the absence of an SO coupling. The formation of symbiotic bright solitons has also been studied in self-repulsive binary BEC mixtures [64, 65] bound by interspecies attraction.

In this paper, using an appropriate mean-field model, we study the properties of different possible quasi-1D solitons in an SO-coupled dipolar pseudo spin-half and spin-one self-repulsive BEC. Using the parameters of the present model, no quasi-1D soliton is possible in the absence of an SO coupling and a dipolar interaction, con-

*sk.adhikari@unesp.br

<https://professores.ift.unesp.br/sk.adhikari/>

sistent with the term self-repulsive. The dipolar atoms are taken to be polarized along the quasi-1D x direction in both pseudo spin-half and spin-one cases. This orientation of polarization leads to an attractive dipolar interaction necessary to bind a self-repulsive BEC to form a soliton, which can freely move along the x direction.

In the case of an SO-coupled dipolar pseudo spin-half BEC, we consider three distinct possibilities for intraspecies and interspecies contact interactions: (i) repulsive intraspecies and interspecies contact interactions, (ii) attractive intraspecies and repulsive interspecies interactions, and (iii) repulsive intraspecies and attractive interspecies interactions. For the above-mentioned interaction (i), for a small strength γ of SO coupling, we have dark-bright, bright-bright and phase-separated bright-bright solitons. [Unless specified to the contrary, in the dark-bright (bright-bright) soliton, the positions of the maxima of density of the bright and the minimum (maximum) of density of dark (bright) components coincide.] In the case of the above-mentioned interaction (ii), for a small γ , we find dark-bright and bright-bright solitons. For a large γ , for the above-mentioned interactions (i) and (ii) we have bright-bright and dark-bright solitons, both with a spatially-periodic stripe modulation in component density with a period of π/γ , in addition to a bright-bright soliton without any modulation in density. In the case of the above-mentioned interaction (iii), both for a small and a large γ , we find only bright-bright solitons.

For an SO-coupled dipolar spin-one BEC, the contact interaction among the three components is governed by two parameters: c_0 and c_2 [29, 32]. Of these, a positive (negative) c_2 corresponds to an anti-ferromagnetic or polar (ferromagnetic) BEC [66]. The properties of a spin-one ferromagnetic BEC could be drastically different from a spin-one anti-ferromagnetic BEC [66] and we consider these two distinct cases in this paper. In the case of an anti-ferromagnetic BEC ($c_2 > 0$), for a small strength γ of SO coupling, one can have the dark-bright-dark and bright-dark-bright quasi-1D solitons, in addition to partially phase-separated bright-bright-bright solitons. [Unless specified to the contrary, in dark-bright-dark, bright-dark-bright and bright-bright-bright solitons, the position of the maximum of density of the bright component coincides with the maximum (minimum) of density of other bright (dark) components.] In the anti-ferromagnetic case, for a large γ , one can have dark-bright-dark and bright-dark-bright quasi-1D solitons with a spatially-periodic modulation in density with the period π/γ . In the case of a ferromagnetic BEC ($c_2 < 0$), for a small strength γ of SO coupling, one can have the formation of overlapping bright-bright-bright solitons and also phase-separated bright-bright-bright solitons. For a large γ , in this case, one can have only bright-bright-bright solitons without any spatially-periodic modulation in density.

The above-mentioned spatially-periodic modulation [39, 67–71] in density in a quasi-1D SO-coupled BEC

soliton is a consequence of the formation of a supersolid [72–76]. A supersolid is a special quantum state of matter with a rigid spatially-periodic crystalline structure [77], breaking continuous translational invariance, that flows with zero viscosity as a superfluid breaking continuous gauge invariance. Spatially-periodic supersolid stripe formation in a quasi-1D pseudo spin-half BEC of ^{23}Na atoms has been experimentally observed [67].

A dark soliton is an excited state and is unstable in general [24]. However, the dark-bright soliton in an SO-coupled pseudo spin-half dipolar BEC and the dark-bright-dark and bright-dark-bright solitons in an SO-coupled spin-one dipolar BEC are dynamically stable. We tested the dynamical stability of these solitons in a pseudo spin-half and a spin-one BEC by real-time propagation over a long time interval using the converged wave function obtained by imaginary-time propagation as the initial state.

In Sec. II A (Sec. II B) we present the mean-field GP equation for the SO-coupled pseudo spin-half (spin-one) dipolar BEC in dimensionless form appropriate for the present study of a quasi-1D soliton. In Sec. III A (Sec. III B) we present an analytic study of the eigenfunctions of the quasi-1D solitons in an SO-coupled pseudo spin-half (spin-one) dipolar BEC. We demonstrate the origin of bright-bright and dark-bright quasi-1D solitons in the pseudo spin-half case. In the spin-one case, possible solitons could be of dark-bright-dark, bright-dark-bright or bright-bright-bright types. In Sec. IV A (Sec. IV B) we present numerical results for the pseudo spin-half (spin-one) case. In Sec. IV C we demonstrate the dynamical stability of these solitons by real-time propagation over a long period of time after introducing a perturbation at time $t = 0$. Finally, in Sec. V we present a brief summary of this investigation.

II. MEAN-FIELD MODEL

We consider a binary (pseudo spin-half) or three-component (spin-one) SO-coupled spinor BEC of N atoms, each of mass m , under a harmonic trap $V(\mathbf{r}) = m\omega_\rho^2(y^2 + z^2)/2 + m\omega_x^2x^2/2$ ($\omega_\rho \gg \omega_x$) of angular frequency ω_x along the x axis and ω_ρ in the quasi-2D y - z plane.

The atomic interaction between two atoms of the ultradilute BEC has two parts: the long-range anisotropic dipolar interaction $V_{\text{dd}}(\mathbf{R})$ and the δ -function contact interaction $\delta(\mathbf{R})$. The intraspecies (V_j , $j = 1, 2$) and interspecies (V_{12}) interactions for two dipolar atoms, polarized along the x axis, placed at positions \mathbf{r} and \mathbf{r}' are given by [40]

$$V_j(\mathbf{R}) = \frac{\mu_0\mu^2}{4\pi}V_{\text{dd}}(\mathbf{R}) + \frac{4\pi\hbar^2a_j}{m}\delta(\mathbf{R}), \quad (1)$$

$$V_{12}(\mathbf{R}) = \frac{\mu_0\mu^2}{4\pi}V_{\text{dd}}(\mathbf{R}) + \frac{4\pi\hbar^2a_{12}}{m}\delta(\mathbf{R}), \quad (2)$$

SPIN-HALF-1-DIP-1dsol

$$V_{\text{dd}}(\mathbf{R}) = \frac{1 - 3 \cos^2 \theta}{\mathbf{R}^3}, \quad (3)$$

where $\mathbf{R} \equiv (\mathbf{r} - \mathbf{r}')$ is the position vector joining the two atoms at \mathbf{r} and \mathbf{r}' , μ_0 is the permeability of free space, μ is the magnetic dipole moment of each atom, θ is the angle made by the vector \mathbf{R} with the polarization x direction, a_j is the intraspecies scattering length of component j , and a_{12} is the interspecies scattering length. To compare the dipolar and contact interactions, the dipolar interaction is expressed in terms of the dipolar length, defined by [40]

$$a_{\text{dd}} \equiv \frac{\mu_0 \mu^2 m}{12\pi \hbar^2}. \quad (4)$$

The dipolar length measures the strength of dipolar interaction in the same way as the scattering length measures the strength of contact interaction in an ultra-dilute BEC. As the different components have the same type of atoms with the same magnetic dipole moment, both intraspecies and the interspecies dipolar interactions and the two (pseudo spin-half BEC) or three (spin-one BEC) possible dipolar lengths are equal.

A. SO-coupled spin-half dipolar GP equation

In cold atoms an artificial synthetic SO coupling is created through the Zeeman interaction $-\boldsymbol{\mu} \cdot \mathbf{B}$ between the magnetic moment $\boldsymbol{\mu}$ of an atom, proportional to its spin $\boldsymbol{\sigma}$, and a magnetic field $\mathbf{B} \sim E_0(-p_y \hat{x} + p_x \hat{y})$ generated in the moving frame [33, 66] of the atom moving with momentum \mathbf{p} , due to an external static electric field $E = E_0 \hat{z}$ in the lab frame. This leads to an SO coupling $-\boldsymbol{\mu} \cdot \mathbf{B} \sim (\sigma_x p_y - \sigma_y p_x)$. The Pauli spin matrices σ_x , σ_y and σ_z are

$$\sigma_x = \begin{pmatrix} 0 & 1 \\ 1 & 0 \end{pmatrix}, \quad \sigma_y = \begin{pmatrix} 0 & -i \\ i & 0 \end{pmatrix}, \quad \sigma_z = \begin{pmatrix} 1 & 0 \\ 0 & -1 \end{pmatrix}, \quad (5)$$

where $i = \sqrt{-1}$. For a strict 1D system moving along x direction, $p_y = 0$ and we can generate an SO coupling of the type $\sigma_y p_x$. Similarly, it is also possible to create an SO coupling of the type $\sigma_x p_x$. The single particle Hamiltonian of the SO-coupled condensate can be written as [33]

$$H_0 = -\frac{\hbar^2}{2m} \nabla_{\mathbf{r}}^2 + V(\mathbf{r}) + \gamma p_x \eta, \quad (6)$$

where $\mathbf{r} \equiv \{x, y, z\}$, $\boldsymbol{\rho} \equiv \{y, z\}$, $\nabla_{\mathbf{r}}^2 = (\partial^2/\partial x^2 + \partial^2/\partial y^2 + \partial^2/\partial z^2) \equiv (\partial_x^2 + \partial_y^2 + \partial_z^2)$, $p_x = -i\hbar \partial_x$ is the momentum along the x axes, γ is the strength of the SO-coupling interaction. We will consider the two possibilities of SO coupling given by $\eta = \sigma_x$ and $\eta = \sigma_y$. Of these two types of SO couplings, the choice $\gamma \sigma_y p_x$ corresponds to an equal mixture of Dresselhaus [78] and Rashba [79, 80] SO

couplings and was realized in the pioneering experiments on SO coupling in a pseudo spin-half BEC of ^{87}Rb [33] and ^{23}Na [34] atoms. We will not consider the choice $\eta = \sigma_z$, as that choice does not permit any off-diagonal coupling and hence does not lead to the variety of solitons found with the choices (5) illustrated in Figs. 1-3 and leads to only bright-bright solitons (result not elaborated in this paper).

This dipolar pseudo spin-half binary BEC, without any synthetic SO coupling, of two components $j = 1, 2$ is described by the following set of equations [40, 81]

$$\begin{aligned} i\hbar \partial_t \phi_j(\mathbf{r}, t) &= \frac{\hbar^2}{m} \left[-\frac{1}{2}(\partial_x^2 + \partial_y^2 + \partial_z^2) \right. \\ &+ \frac{m^2}{2\hbar^2} (\omega_\rho^2 \rho^2 + \omega_x^2 x^2) \\ &+ 4\pi a_j N_j |\phi_j(\mathbf{r}, t)|^2 + 4\pi a_{12} N_k |\phi_k(\mathbf{r}, t)|^2 \\ &+ 3a_{\text{dd}} N_j \int V_{\text{dd}}(\mathbf{R}) |\phi_j(\mathbf{r}', t)|^2 d\mathbf{r}' \\ &+ \left. 3a_{\text{dd}} N_k \int V_{\text{dd}}(\mathbf{R}) |\phi_k(\mathbf{r}', t)|^2 d\mathbf{r}' \right] \phi_j(\mathbf{r}, t), \\ j &\neq k = 1, 2, \end{aligned} \quad (7)$$

where $\partial_t \equiv \partial/\partial t$, N_j and N_k are the number of atoms in the two components j and k , respectively ($N = N_1 + N_2$). Here $j = 1$ is the spin-up component and $j = 2$ is the spin-down component. Equations (7) can be cast in the following dimensionless form if we scale lengths in units of the harmonic oscillator length $l_0 = \sqrt{\hbar/m\omega_\rho}$, time units of $t_0 = 1/\omega_\rho$, density $|\phi_j|^2$ in units of l_0^{-3} , and energy in units of $\hbar\omega_\rho$

$$\begin{aligned} i\partial_t \phi_j(\mathbf{r}, t) &= \left[-\frac{1}{2}(\partial_x^2 + \partial_y^2 + \partial_z^2) + \frac{1}{2} \left(\rho^2 + \frac{\omega_x^2}{\omega_\rho^2} x^2 \right) \right. \\ &+ 4\pi a_j N_j |\phi_j(\mathbf{r}, t)|^2 + 4\pi a_{12} N_k |\phi_k(\mathbf{r}, t)|^2 \\ &+ 3a_{\text{dd}} N_j \int V_{\text{dd}}(\mathbf{R}) |\phi_j(\mathbf{r}', t)|^2 d\mathbf{r}' \\ &+ \left. 3a_{\text{dd}} N_k \int V_{\text{dd}}(\mathbf{R}) |\phi_k(\mathbf{r}', t)|^2 d\mathbf{r}' \right] \phi_j(\mathbf{r}, t), \\ j &\neq k = 1, 2. \end{aligned} \quad (8)$$

Without any risk of confusion, here and in the following we are using the same symbols to denote the scaled dimensionless and unscaled variables.

We consider a quasi-1D pseudo spin-half dipolar BEC with a strong trap in the y - z plane. We assume that the dynamics of the BEC in the y - z plane is frozen in the ground state

$$\psi_B(\boldsymbol{\rho}) = \pi^{-1/2} e^{-\rho^2/2}, \quad \rho^2 = y^2 + z^2, \quad (9)$$

and the relevant dynamics of the BEC will be confined along the polarization x direction. In this case it is possible to integrate out the y and z variables and write a set of coupled equations for the relevant dynamics along the x direction. The component wave function of the

BEC can be written as

$$\phi_j(\mathbf{r}, t) = \psi_B(\rho) \times \psi_j(x, t), \quad (10)$$

where the wave function $\psi_j(x, t)$ describes the relevant dynamics of the quasi-1D BEC confined along the x direction. To obtain the relevant dynamics, we substitute Eq. (10) into Eq. (8), multiply the resultant equation by $\psi_B(\rho)$ and integrate over $\rho \equiv \{y, z\}$ [82]. To avoid the difficulty associated with the integration over the divergent dipolar interaction in configuration space, this integral is conveniently evaluated in the momentum space. This procedure leads to the following set of quasi-1D GP equations for the two components [81, 83] of the pseudo spin-half SO-coupled dipolar BEC soliton

$$i\partial_t \psi_j(x, t) = \left[-\frac{1}{2} \partial_x^2 + c_0 n_j(x, t) + c_2 n_k(x, t) + d \sum_{j=1,2} s_j(x, t) \right] \psi_j(x, t) + [\gamma p_x \eta \psi(x, t)]_j, \quad (11)$$

$$s_j(x, t) = \int \frac{dk_x}{2\pi} e^{-ik_x x} \tilde{n}_j(k_x, t) h_{1D} \left(\frac{k_x}{\sqrt{2}} \right), \quad (12)$$

$$h_{1D} \left(\frac{k_x}{\sqrt{2}} \right) = \frac{1}{(2\pi)^2} \int d\mathbf{k}_\rho \left(\frac{3k_x^2}{k^2} - 1 \right) |\tilde{n}(\mathbf{k}_\rho)|^2 = \frac{1}{2\pi} \int_0^\infty du \left[\frac{3k_x^2}{2u + 3k_x^2} - 1 \right] e^{-u}, \quad (13)$$

where $\tilde{n}_j(k_x, t)$ and $\tilde{n}(\mathbf{k}_\rho)$ are the Fourier transformations of densities $|\psi_j(x, t)|^2$ and $\tilde{n}(\mathbf{k}_\rho)$, respectively, and are given by

$$\tilde{n}_j(k_x, t) = \int_{-\infty}^\infty e^{ik_x x} |\psi_j(x, t)|^2 dx, \quad (14)$$

$$\tilde{n}(\mathbf{k}_\rho) = \int e^{i\mathbf{k}_\rho \cdot \rho} |\psi_B(\rho)|^2 d\rho = e^{-k_\rho^2/4}, \quad (15)$$

where $k_\rho = \sqrt{k_y^2 + k_z^2}$, and we have included the SO-coupling term in Eq. (11) and assumed that $a_1 = a_2 \equiv a$. The dipolar intraspecies or interspecies nonlinearity $d = 4\pi a_{\text{dd}} N$, intraspecies contact nonlinearity $c_0 = 2Na$, interspecies contact nonlinearity $c_2 = 2Na_{12}$. The chosen interaction parameters will be such that there could be no solitons in the absence of SO coupling and dipolar interaction. Here $n_j(x, t) = |\psi_j(x, t)|^2$, $j = 1, 2$ are the densities of the two components, and $n(x, t) = \sum_j n_j(x, t)$ the total density. In Eq. (11), for $\eta = \sigma_x$,

$$[\gamma p_x \eta \psi(x, t)]_j = -i\gamma \partial_x \psi_k(x, t), \quad j \neq k, \quad (16)$$

and for $\eta = \sigma_y$,

$$[\gamma p_x \eta \psi(x, t)]_j = (-1)^k \gamma \partial_x \psi_2(x, t), \quad j \neq k, \quad (17)$$

$j, k = 1, 2$. In this study of quasi-1D solitons along the x direction we have dropped the harmonic oscillator trapping potential from Eq. (11). The normalization condition on the total density is

$$\int_{-\infty}^\infty n(x, t) dx = 1. \quad (18)$$

The SO coupling allows a transfer of atoms from one component to another so that there is no condition of normalization on the individual components. The imbalance between the spin-up and spin-down components is measured by magnetization \mathcal{M} , defined by

$$\mathcal{M} = \frac{\int_{-\infty}^\infty dx [n_1(x) - n_2(x)]}{\int_{-\infty}^\infty dx [n_1(x) + n_2(x)]}. \quad (19)$$

Imaginary-time propagation does not conserve normalization automatically. In each time iteration the total normalization is adjusted to unity, and the normalization of the individual components is allowed to vary freely with time propagation. Imaginary-time propagation settles the final converged density of the components and the final magnetization \mathcal{M} .

B. SO-coupled spin-one dipolar GP equation

In this case the mean-field equations are similar to those of a pseudo spin-half SO-coupled dipolar BEC and we highlight the differences from the pseudo spin-half case. Here the SO-coupled spinor BEC has three components $j = 1, 2, 3$ in contrast to a pseudo spin-half BEC with two components $j = 1, 2$. Again, $j = 1$ represents spin-up component and $j = 2$ represents the spin-down component. We will consider the same SO-coupling interaction in this case as in the case of an SO-coupled pseudo spin-half dipolar BEC in Sec. II A. The single-particle Hamiltonian is now given by

$$H_0 = -\frac{\hbar^2}{2m} (\partial_x^2 + \partial_y^2 + \partial_z^2) + V(\mathbf{r}) + \gamma p_x \eta. \quad (20)$$

However, the spin operator now has three spin components and the spin-one matrices are 3×3 matrices. For η we now consider the two possibilities $\eta = \Sigma_x$ and Σ_y , where

$$\Sigma_x = \frac{1}{\sqrt{2}} \begin{pmatrix} 0 & 1 & 0 \\ 1 & 0 & 1 \\ 0 & 1 & 0 \end{pmatrix}, \quad \Sigma_y = \frac{1}{\sqrt{2}} \begin{pmatrix} 0 & -i & 0 \\ i & 0 & -i \\ 0 & i & 0 \end{pmatrix}, \quad (21)$$

corresponding to the SO coupling $\gamma p_x \Sigma_x$ and $\gamma p_x \Sigma_y$, respectively. We will not consider the possibility

$$\Sigma_z = \begin{pmatrix} 1 & 0 & 0 \\ 0 & 0 & 0 \\ 0 & 0 & -1 \end{pmatrix}, \quad (22)$$

where there is no off-diagonal coupling. Consequently, the choice (22) does not lead to the variety of solitons found with the choices (21), illustrated in Figs. 4-5, and leads only to bright-bright-bright solitons.

The quasi-1D equations for the three components of a SO-coupled spin-one BEC are well known [38, 66], e.g., Eqs. (23)-(25) with $d = \gamma = 0$. For a dipolar BEC

($d \neq 0$) the dipole-dipole interaction terms are introduced in these equations as in the case of a pseudo spin-half system, viz. Eq. (11). The resultant quasi-1D equations for a dipolar spin-one SO-coupled BEC of N atoms can be obtained by combining the same of a dipolar BEC [83] with that of a spin-one BEC [38, 84, 85] and are as follows

$$i\partial_t\psi_1(x,t) = \left[-\frac{\partial_x^2}{2} + c_0n(x,t) + c_2\{n_1(x,t) + n_2(x,t) - n_3(x,t)\} + d\sum_{j=1}^3 s_j(x,t) \right] \psi_1(x,t) + c_2\psi_2^2(x,t)\psi_3^*(x,t) + [\gamma p_x \eta \psi(x,t)]_1, \quad (23)$$

$$i\partial_t\psi_2(x,t) = \left[-\frac{\partial_x^2}{2} + c_0n(x,t) + c_2\{n_1(x,t) + n_3(x,t)\} + d\sum_{j=1}^3 s_j(x,t) \right] \psi_2(x,t) + 2c_2\psi_1(x,t)\psi_3(x,t) \times \psi_2^*(x,t) + [\gamma p_x \eta \psi(x,t)]_2, \quad (24)$$

$$i\partial_t\psi_3(x,t) = \left[-\frac{\partial_x^2}{2} + c_0n(x,t) + c_2\{n_3(x,t) + n_2(x,t) - n_1(x,t)\} + d\sum_{j=1}^3 s_j(x,t) \right] \psi_3(x,t) + c_2\psi_2^2(x,t)\psi_1^*(x,t) + [\gamma p_x \eta \psi(x,t)]_3, \quad (25)$$

where we have introduced the SO-coupling terms $[\gamma p_x \eta \psi(x,t)]_j$, $j = 1, 2, 3$. Here the spin-one interaction parameters are [38, 66] $c_0 = 2N(a_0 + 2a_2)/l_0$, $c_2 = 2N(a_2 - a_0)/l_0$, a_0 and a_2 are the s -wave scattering lengths of two spin-one atoms in the total spin 0 and 2 channels. For a ferromagnetic BEC $c_2 < 0$ and for an anti-ferromagnetic BEC $c_2 > 0$ [66]. In this study we will consider $c_0 > 0$ and a small $|c_2|$, including both ferromagnetic and anti-ferromagnetic domains. For this choice of c_0 and c_2 , there cannot be any solitons in the absence of the dipolar interaction and SO-coupling; we will term such a BEC as self-repulsive indicating that the net contact interaction is repulsive, although c_2 can have a small negative value in the ferromagnetic domain ($|c_0| > |c_2|$). For a spin-one BEC, the background scattering lengths of ^{87}Rb and ^{23}Na atoms fall in the ferromagnetic [86–88] and anti-ferromagnetic [89] domains, respectively. In Eqs. (23)-(25), for $\eta = \Sigma_x$,

$$[\gamma p_x \eta \psi(x,t)]_j = -\frac{i}{\sqrt{2}}\gamma\partial_x\psi_2(x,t), \quad j = 1, 3, \quad (26)$$

$$[\gamma p_x \eta \psi(x,t)]_2 = -\frac{i}{\sqrt{2}}\gamma[\partial_x\psi_1(x,t) + \partial_x\psi_3(x,t)], \quad (27)$$

and for $\eta = \Sigma_y$,

$$[\gamma p_x \eta \psi(x,t)]_j = \frac{(-1)^j}{\sqrt{2}}\gamma\partial_x\psi_2(x,t), \quad j = 1, 3, \quad (28)$$

$$[\gamma p_x \eta \psi(x,t)]_2 = \frac{1}{\sqrt{2}}\gamma[\partial_x\psi_1(x,t) - \partial_x\psi_3(x,t)]. \quad (29)$$

In this case also the normalization of individual components is not conserved and only the total normalization of the three components is conserved. The magnetization

$$\mathcal{M} = \frac{\int_{-\infty}^{\infty} dx[n_1(x) - n_3(x)]}{\int_{-\infty}^{\infty} dx[n_1(x) + n_2(x) + n_3(x)]}, \quad (30)$$

gives a measure of the disbalance between the spin-up and spin-down components.

III. ANALYTICAL RESULTS

A. SO-coupled spin-half GP equation

Equations (11) can be derived from the energy functional

$$E[\psi_j] = \frac{1}{2} \int_{-\infty}^{\infty} dx [\sum_{j=1}^2 |\partial_x \psi_j|^2 + c_0(n_1^2 + n_2^2) + 2c_2n_1n_2 + d(s_1 + s_2)n - 2i\psi^T \gamma \partial_x \eta \psi], \quad (31)$$

where $\psi^T = (\psi_1, \psi_2)$, using the variational rule [27]

$$i\partial_t\psi_j = \frac{\delta E[\psi_j]}{\delta \psi_j^*}. \quad (32)$$

Many properties of a pseudo spin-half, nondipolar or dipolar, SO-coupled uniform BEC can be understood from a consideration of the eigenfunction-eigenvalue problem of the linear Hamiltonian, setting all nondipolar and dipolar nonlinear interactions and the confining trap to zero [$c_0 = c_2 = d = V(x) = 0$] [38]. The quasi-1D stationary wave function of the linear single-particle trap-less Hamiltonian corresponding to Eq. (11) is

$$H_0^{1D} = -\frac{1}{2}\partial_x^2 - i\gamma\partial_x\eta, \quad (33)$$

which for $\eta = \sigma_x$ satisfies the following eigenfunction-eigenvalue problem for a stationary state

$$\begin{pmatrix} -\frac{1}{2}\partial_x^2 & -i\gamma\partial_x \\ -i\gamma\partial_x & -\frac{1}{2}\partial_x^2 \end{pmatrix} \begin{pmatrix} \psi_1(x) \\ \psi_2(x) \end{pmatrix} = \mathcal{E} \begin{pmatrix} \psi_1(x) \\ \psi_2(x) \end{pmatrix}, \quad (34)$$

which has the following two degenerate eigenfunctions with the eigenvalue $\mathcal{E} = -\gamma^2/2$:

$$\begin{pmatrix} \psi_1(x) \\ \psi_2(x) \end{pmatrix} = \begin{pmatrix} \cos(\gamma x) \\ -i\sin(\gamma x) \end{pmatrix}, \quad \begin{pmatrix} \psi_1(x) \\ \psi_2(x) \end{pmatrix} = \begin{pmatrix} \sin(\gamma x) \\ i\cos(\gamma x) \end{pmatrix}. \quad (35)$$

For $\eta = \sigma_y$ we have the following eigenfunction-eigenvalue problem

$$\begin{pmatrix} -\frac{1}{2}\partial_x^2 & -\gamma\partial_x \\ +\gamma\partial_x & -\frac{1}{2}\partial_x^2 \end{pmatrix} \begin{pmatrix} \psi_1(x) \\ \psi_2(x) \end{pmatrix} = \mathcal{E} \begin{pmatrix} \psi_1(x) \\ \psi_2(x) \end{pmatrix}, \quad (36)$$

which has the following two degenerate eigenfunctions with the eigenvalue $\mathcal{E} = -\gamma^2/2$:

$$\begin{pmatrix} \psi_1(x) \\ \psi_2(x) \end{pmatrix} = \begin{pmatrix} \cos(\gamma x) \\ \sin(\gamma x) \end{pmatrix}, \quad \begin{pmatrix} \psi_1(x) \\ \psi_2(x) \end{pmatrix} = \begin{pmatrix} \sin(\gamma x) \\ -\cos(\gamma x) \end{pmatrix}. \quad (37)$$

In both cases, $\eta = \sigma_x, \sigma_y$, we find from Eqs. (35) and (37) that the energy and the densities are the same, although the wave functions are different. The density of the two components has a spatially-periodic modulation, given by $\sin^2(\gamma x)$ and $\cos^2(\gamma x)$, along the quasi-1D x direction with a period of π/γ ; however, the total density does not have this modulation and $|\psi_1(x)|^2 + |\psi_2(x)|^2 = 1$. The two component densities have a maximum and a minimum at the origin $x = 0$ leading to a dark-bright soliton in the uniform system.

B. SO-coupled spin-one GP equation

The time-independent version of Eqs. (23)-(25), appropriate for the stationary solutions, can be derived from the energy functional

$$E[\psi_j] = \frac{1}{2} \int_{-\infty}^{\infty} dx \left[\sum_{j=1}^3 |\partial_x \psi_j|^2 + c_0 n^2 + c_2 \{n_1^2 + n_3^2 + 2(n_1 n_2 + n_3 n_2 - n_1 n_3 + \psi_3^* \psi_2^2 \psi_1^* + \psi_3 \psi_2^{*2} \psi_1)\} + d(s_1 + s_2 + s_3)n - 2i\psi^T \gamma \partial_x \eta \psi \right], \quad (38)$$

using the variational rule (32), where now $\psi^T = (\psi_1, \psi_2, \psi_3)$.

Again, many properties of a spin-one SO-coupled uniform BEC can be understood from a consideration of the eigenfunction-eigenvalue problem of the linear Hamiltonian, setting all nondipolar and dipolar nonlinear interactions and the confining trap to zero [$c_0 = c_2 = d = V(x) = 0$] [38]. The quasi-1D stationary wave function of the linear single-particle trap-less Hamiltonian corresponding to Eqs. (23)-(25)

$$H_0^{1D} = -\frac{1}{2} \partial_x^2 - i\gamma \partial_x \eta, \quad (39)$$

which, for $\eta = \Sigma_x$, satisfies the following eigenfunction-eigenvalue problem

$$\begin{pmatrix} -\frac{1}{2} \partial_x^2 & -\frac{i}{\sqrt{2}} \gamma \partial_x & 0 \\ -\frac{i}{\sqrt{2}} \gamma \partial_x & -\frac{1}{2} \partial_x^2 & -\frac{i}{\sqrt{2}} \gamma \partial_x \\ 0 & -\frac{i}{\sqrt{2}} \gamma \partial_x & -\frac{1}{2} \partial_x^2 \end{pmatrix} \begin{pmatrix} \psi_1(x) \\ \psi_2(x) \\ \psi_3(x) \end{pmatrix} = \mathcal{E} \begin{pmatrix} \psi_1(x) \\ \psi_2(x) \\ \psi_3(x) \end{pmatrix}, \quad (40)$$

which has the following two linearly independent degenerate eigenfunctions with energy $\mathcal{E} = -\gamma^2/2$:

$$\begin{pmatrix} \psi_1(x) \\ \psi_2(x) \\ \psi_3(x) \end{pmatrix} = \frac{1}{\sqrt{2}} \begin{pmatrix} \cos(\gamma x) \\ -i\sqrt{2} \sin(\gamma x) \\ \cos(\gamma x) \end{pmatrix}, \quad (41)$$

$$\begin{pmatrix} \psi_1(x) \\ \psi_2(x) \\ \psi_3(x) \end{pmatrix} = \frac{1}{\sqrt{2}} \begin{pmatrix} \sin(\gamma x) \\ i\sqrt{2} \cos(\gamma x) \\ \sin(\gamma x) \end{pmatrix}. \quad (42)$$

For $\eta = \Sigma_y$, we have the following eigenfunction-

eigenvalue problem

$$\begin{pmatrix} -\frac{1}{2} \partial_x^2 & -\frac{1}{\sqrt{2}} \gamma \partial_x & 0 \\ \frac{1}{\sqrt{2}} \gamma \partial_x & -\frac{1}{2} \partial_x^2 & -\frac{1}{\sqrt{2}} \gamma \partial_x \\ 0 & \frac{1}{\sqrt{2}} \gamma \partial_x & -\frac{1}{2} \partial_x^2 \end{pmatrix} \begin{pmatrix} \psi_1(x) \\ \psi_2(x) \\ \psi_3(x) \end{pmatrix} = \mathcal{E} \begin{pmatrix} \psi_1(x) \\ \psi_2(x) \\ \psi_3(x) \end{pmatrix}, \quad (43)$$

which has the following two degenerate eigenfunctions with eigenvalue $\mathcal{E} = -\gamma^2/2$:

$$\begin{pmatrix} \psi_1(x) \\ \psi_2(x) \\ \psi_3(x) \end{pmatrix} = \frac{1}{\sqrt{2}} \begin{pmatrix} \cos(\gamma x) \\ \sqrt{2} \sin(\gamma x) \\ -\cos(\gamma x) \end{pmatrix}, \quad (44)$$

$$\begin{pmatrix} \psi_1(x) \\ \psi_2(x) \\ \psi_3(x) \end{pmatrix} = \frac{1}{\sqrt{2}} \begin{pmatrix} \sin(\gamma x) \\ -\sqrt{2} \cos(\gamma x) \\ -\sin(\gamma x) \end{pmatrix}. \quad (45)$$

The densities corresponding to eigenfunctions (41) and (42) are identical to the same of eigenfunctions (44) and (45). These densities correspond to a spatially periodic sinusoidal stripe along the x axis with a period of π/γ ; the stripe pattern of components $j = 1$ and 3 is always the same and that of component $j = 2$ is always displaced with respect to the former. The former may have a maximum (minimum) at the origin $x = 0$, where the latter has a minimum (maximum) leading to a bright-dark-bright or a dark-bright-dark soliton, respectively, in a uniform system. The total density of the three components do not have any modulation in density and is uniform in nature: $|\psi_1(x)|^2 + |\psi_2(x)|^2 + |\psi_3(x)|^2 = 1$. The solutions presented in Secs. III A and III B of the linear equations are not localized. We will see in Sec. IV, the localized solitons of the full nonlinear equations have the same modulation in density.

IV. NUMERICAL RESULT

To solve the binary equations (11) for a quasi-1D SO-coupled pseudo spin-half dipolar BEC and three-component equations (23)-(25) for a quasi-1D SO-coupled spin-one dipolar BEC numerically, we propagate these in time by the split-time-step Crank-Nicolson discretization scheme [90]. In this study of solitons in an SO-coupled dipolar pseudo spin-half or spin-one BEC, all the (contact and dipolar) interaction parameters will be taken to be very small in magnitude, so that the system remains in the very weak-coupling limit [27], where beyond-mean-field effects are negligibly small and not of concern, even in the presence of dipolar interaction. On the other extreme of very strong-coupling limit of droplet formation in a dipolar BEC, quantum-fluctuation effects are highly relevant and are incorporated in the mean-field model through the higher-order Lee-Huang-Yang interaction [91], or one can also employ different beyond-mean-field formulations. As we require to solve the GP equation in the presence of both SO-coupling and dipolar interaction, we needed to combine the Open Multiprocessing Programs for solving the dipolar [92] and SO-coupled

[93] GP equations. We employ the space step $dx = 0.1$ and the time step $dt = dx^2 \times 0.1$ for imaginary-time propagation and the time step $dt = dx^2 \times 0.025$ for real-time propagation. In all calculations of stationary states, we use imaginary-time propagation with the conservation of total normalization during time propagation, which finds the lowest-energy solution of each type. The real-time propagation is used to demonstrate the dynamical stability of the solitons.

In the presence of SO coupling, the transfer of atoms from one spin component to another is allowed [66] and the number of atoms in each component is not separately conserved. Consequently, the magnetization \mathcal{M} is not a good quantum number in the presence of SO coupling. Hence the magnetization as well as the normalization of individual components is not conserved during imaginary-time propagation. As the total number of atoms in all the components is conserved, the conservation of total normalization is enforced in each time step of imaginary-time propagation. In addition, if necessary, the conservation of magnetization in each time step can be enforced as in Ref. [38]. Some of the present solitons are possible for a zero as well as a nonzero value of magnetization \mathcal{M} ; in those cases we present the soliton with zero magnetization in this paper. For a dark-bright soliton in the case of a pseudo spin-half dipolar BEC, the magnetization is intrinsically non-zero; in that case we illustrate the ground state with $M \neq 0$ obtained by the imaginary-time propagation.

A. Quasi-1D SO-coupled spin-half self-repulsive dipolar BEC soliton

We study the formation of different types of solitons in a quasi-1D SO-coupled pseudo spin-half self-repulsive dipolar BEC. In this system we will choose the intraspecies and interspecies scattering lengths in such a way that no solitons are possible in the absence of a dipolar interaction and an SO coupling. Both a dipolar interaction [83] and an SO coupling [61] contribute to an attraction in the system and these help to form a bound soliton. We will consider three possibilities of intraspecies and interspecies interactions: repulsive intraspecies and interspecies contact interactions, attractive intraspecies and repulsive interspecies contact interactions, and repulsive intraspecies and attractive interspecies contact interactions.

Without losing generality, first we consider a dipolar BEC with a small value of the nonlinearity parameters $c_0 = c_2 = 0.5, d = 2$ in Eq. (11), corresponding to a repulsive intraspecies and also a repulsive interspecies contact interaction. In this case, due to a moderate dipolar interaction, a soliton can be formed for a small value of the SO-coupling strength γ , which facilitates both theoretical and numerical investigations. For a small γ ($\gamma = 0.1$) we find the following three types of quasi-1D solitons in a self-repulsive dipolar BEC: a dark-bright

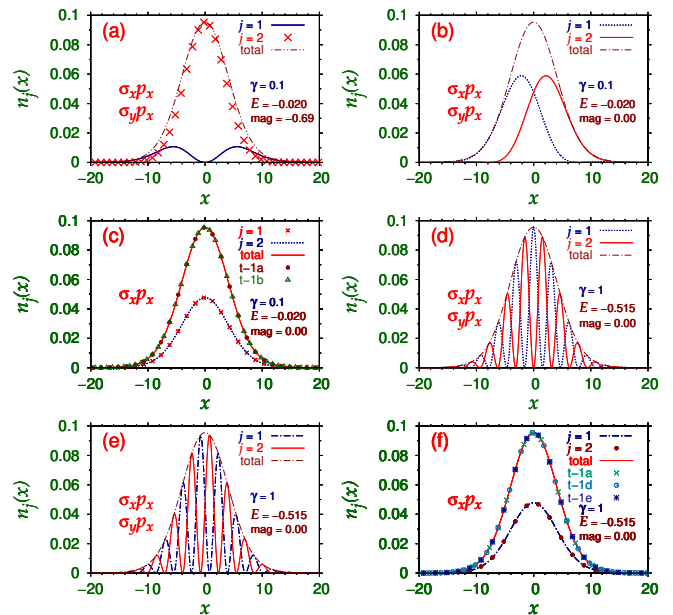


FIG. 1: (Color online) Density of components $j = 1, 2$ and total density of a quasi-1D SO-coupled pseudo spin-half dipolar (a) dark-bright, (b) a phase-separated bright-bright, and (c) a bright-bright soliton for SO-coupling strength $\gamma = 0.1$. In (c) we also show the total density of the solitons in plots (a) (t-1a) and (b) (t-1b). The plots (d)-(f) display a dark-bright, a phase-separated bright-bright, and a bright-bright soliton, for $\gamma = 1$, with the first two having a spatially-periodic modulation in density. The energy (E), magnetization (mag), and γ are given in the inset of all plots of this paper. The parameters are $c_0 = c_2 = 0.5, d = 2$. All quantities in this and following figures are dimensionless and the total density is always normalized to unity, viz. Eq. (18).

soliton, an overlapping and a phase-separated bright-bright soliton. In Fig. 1 we present the component and total density of a quasi-1D SO-coupled pseudo spin-half dipolar (a) dark-bright, (b) a phase-separated bright-bright, and (c) a bright-bright soliton for SO-coupling strength $\gamma = 0.1$ and SO couplings $\gamma\sigma_x p_x$ and $\gamma\sigma_y p_x$. The bright (dark) soliton component has a maximum (minimum of zero) of density at the center. However, the wave function in the presence of SO coupling is complex and in all dark soliton components illustrated in this paper, at the central zero of density, there is a phase jump of π , as in any dark soliton [23]. The bright-bright soliton of Fig. 1(c) is possible only for SO-coupling $\gamma\sigma_x p_x$. These three solitons are quasi-degenerate with energy $E = -0.020$. We use the term quasi-degenerate, as the degeneracy is established only numerically. Also, we verified that the degeneracy is removed for a slightly larger value of the nonlinearities. The total density n of the solitons in Figs. 1(a)-(c) are equal as can be seen in Fig. 1(c), where we also plotted the total density n of the solitons of Figs. 1(a)-(b). As we have different types of solitons for different (intraspecies and interspecies) interaction parameters, these results are summarized in a

tabular form in Table I, clearly indicating which types of solitons emerge in the different parameter regimes for both pseudo spin-half and spin-one dipolar BEC.

TABLE I: Different types of soliton for dipolar spin-half and spin-one BECs: dark-bright (d-b), bright-bright (b-b), phase-separated bright-bright (ph-sep b-b), dark-bright-dark (d-b-d), bright-dark-bright (b-d-b), bright-bright-bright (b-b-b). The qualifier “(m)” denotes a spatially periodic modulation in density of all components. The dipolar interaction parameter in all cases is $d = 2$.

Spin	γ	c_0, c_2	Type of soliton
1/2	0.1	$c_0 = 0.5, c_2 = 0.5$	d-b, ph-sep b-b, b-b
		$c_0 = -0.5, c_2 = 0.5$	d-b, b-b
		$c_0 = 0.5, c_2 = -0.5$	b-b
1/2	1	$c_0 = 0.5, c_2 = 0.5$	d-b (m), b-b (m), b-b
		$c_0 = -0.5, c_2 = 0.5$	d-b (m), b-b (m), b-b
		$c_0 = 0.5, c_2 = -0.5$	b-b
1	0.1	$c_0 = 0.5, c_2 = 0.5$	ph-sep b-b-b, d-b-d, b-d-b
		$c_0 = 0.5, c_2 = -0.1$	b-b-b, ph-sep b-b-b
1	1	$c_0 = 0.5, c_2 = 0.5$	d-b-d (m), b-d-b (m)
		$c_0 = 0.5, c_2 = -0.1$	b-b-b

As the SO-coupling strength γ is increased, the scenario of soliton formation changes; the three solitons of Figs. 1(a)-(c) evolve into the three solitons of Figs. 1(d)-(f), respectively. For $\gamma = 1$ the linear density of the dark-bright soliton and the phase-separated bright-bright soliton develops a spatially-periodic modulation with the period π/γ as illustrated in Figs. 1(d)-(e), respectively. In these cases the total density has a smooth behavior without any spatial modulation. The density pattern of the overlapping bright-bright soliton remains the same as γ is increased from 0.1 to 1, as illustrated in Figs. 1(c) and 1(f). The three solitons of Figs. 1(d)-(f) are quasi-degenerate with energy $E = -0.515$. We could not find any other state for these parameters. Now we find that the total density of all the solitons in Figs. 1(a)-(f) are equal as can be seen from Figs. 1(f), where we also plotted the total density of solitons of Figs. 1(a) and 1(d)-(e). For a small $\gamma (\lesssim 1)$, and small nonlinearities c_0, c_2, d , the degenerate ground states all have the same total density. This could be possible if the energy is a function of the total density. We verified that if c_0 and c_2 are different the degeneracy of the states for a fixed γ will be removed and the solitons will not have the same total density. As we are using $c_0 = c_2$, using Eq. (12) the energy (31) can be written as

$$E = \frac{1}{2} \int_{-\infty}^{\infty} dx \left[\left\{ \sum_{j=1}^2 |\partial_x \psi_j(x)|^2 - 2i\psi^T(x)\gamma\partial_x\eta\psi(x) \right\} + \{c_0 n^2(x) + ds(x)n(x)\} \right], \quad (46)$$

where

$$s(x) = \int \frac{dk_x}{2\pi} e^{-ik_x x} \tilde{n}(k_x) h_{1D} \left(\frac{k_x}{\sqrt{2}} \right). \quad (47)$$

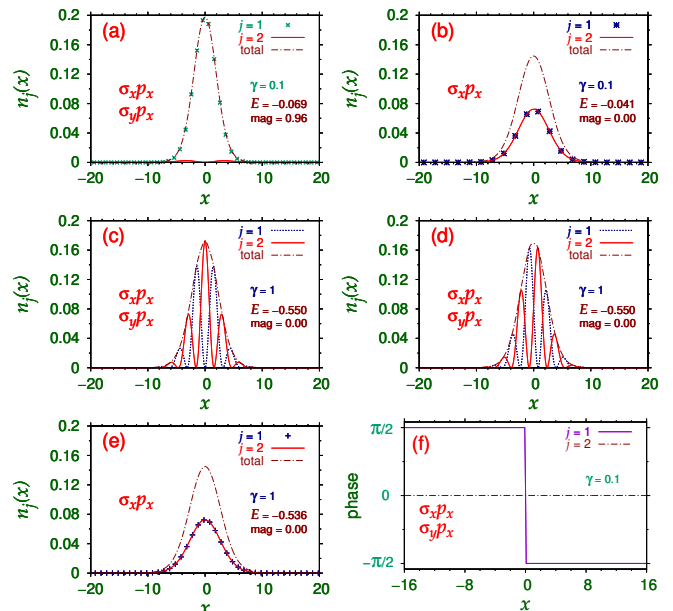


FIG. 2: Density of components $j = 1, 2$ and total density of a quasi-1D SO-coupled pseudo spin-half dipolar (a) dark-bright, and (b) bright-bright soliton for SO-coupling strength $\gamma = 0.1$. The plots (c)-(e) display a dark-bright, a phase-separated bright-bright, and a bright-bright soliton, respectively for $\gamma = 1$. The plot (f) presents the phase of the wave functions of the dark-bright soliton of plot (a). The parameters are $c_0 = -0.5, c_2 = 0.5, d = 2$.

The energy (46) has two parts. The first part in the first curly bracket of this expression is the single-particle linear Hamiltonian (33), which contributes $E_1 = -\gamma^2/2$ to energy as found in Sec. III A. The nonlinear interaction part in the second curly bracket of Eq. (46) is a function of total density n , contributes an amount E_2 , independent of γ , to total energy $E (= E_1 + E_2)$. This provides a qualitative explanation of the fact that all the degenerate states of Fig. 1 have the same total density. From the quasi-degenerate states of Figs. 1(a)-(c), with $\gamma = 0.1$ and $E = -0.020$, we can estimate $E_2 = E - E_1 = -0.020 + \gamma^2/2 = -0.015$. Using this γ -independent estimate for E_2 we can now analytically predict the energy E of the three quasi-degenerate states of Figs. 1(d)-(f) for $\gamma = 1$ to be $E = -\gamma^2/2 + E_2 = -0.515$ in agreement with the numerical result $E = -0.515$ of the solitons in Figs. 1(d)-(f).

However, the above breakup of energy E in γ -dependent linear part E_1 and a γ -independent nonlinear part E_2 , viz. Eq. (40), is always possible, for the small values of the nonlinearities used in this paper, where, in general, E_2 will be a function of the component densities. If, for two states, the component densities are equal, these states should be degenerate if γ is the same. However, if γ of the two states is different, the energy of the two states are related by a simple algebraic relation

$$E^{(2)} = E^{(1)} - \frac{\gamma_2^2}{2} + \frac{\gamma_1^2}{2}, \quad (48)$$

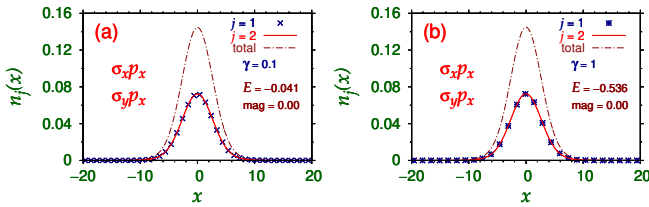


FIG. 3: Density of components $j = 1, 2$ and total density of a quasi-1D SO-coupled pseudo spin-half dipolar bright-bright soliton for (a) $\gamma = 0.1$ and (b) $\gamma = 1$. The parameters are $c_0 = 0.5, c_2 = -0.5, d = 2$.

where $E^{(2)}$ and $E^{(1)}$ are the energies of two states with equal component densities for $\gamma = \gamma_2$ and γ_1 , respectively. The relation (48) is valid whenever the energy can be broken into two parts, and not only in the case of a pseudo spin-half BEC.

To study the case of an attractive intraspecies interaction and a repulsive interspecies interaction we consider the parameters $c_0 = -0.5, c_2 = 0.5, d = 2$. Although, the intraspecies interaction is attractive, in the absence of a dipolar interaction ($d = 0$), and an SO coupling, there is no binary soliton formation in this case for the present set of parameters. However, there could be a separate (uncoupled) single-component soliton(s). For $\gamma = 0.1$ we have the same dark-bright and bright-bright solitons, viz. Figs. 1(a) and 1(c), as illustrated in Figs. 2(a)-(b), in increasing order of energy. The soliton in Fig. 2(b) is in an excited metastable state. As $c_0 \neq c_2$ in this case, the total densities and energies of the solitons in Figs. 2(a)-(b) are different. In the case of the dark-bright soliton of Fig. 2(a), the magnetization is almost unity ($|\mathcal{M}| = 0.97 \approx 1$) indicating a very small number of atoms in the dark soliton component. However, the phase-separated bright-bright soliton of the type presented in Fig. 1(b) is not possible in this case for $\gamma = 0.1$. For $\gamma = 1$ we have (the same three types of solitons as presented in Fig. 1): the dark-bright, the phase-separated bright-bright and the overlapping bright-bright solitons, as illustrated in Figs. 2(c)-(e), respectively. Again, the dark-bright and phase-separated bright-bright solitons shown in Figs. 2(c)-(d) are quasi-degenerate ground states and have a spatially-periodic modulation in density, whereas the overlapping bright-bright soliton of Fig. 2(e) is an excited metastable state. The bright-bright solitons of Figs. 2(b) and 2(e) are possible only for SO coupling $\gamma\sigma_x p_x$ and not for $\gamma\sigma_y p_x$. In this case the component and total densities of the solitons in Figs. 2(b) and 2(e) for $\gamma_1 = 0.1$ and $\gamma_2 = 1$, respectively, are identical and the two energies $E_1 = -0.041$ and $E_2 = -0.536$ satisfy the relation (48). In Fig. 2(f) we plot the phase of the wave function of the two components of the dark-bright soliton presented in Fig. 2(a). As expected [23], the phase of the dark component shows a jump of π at the origin while that of the bright component is zero. In fact, there is such a jump whenever there is a zero in the wave function leading to many such jumps in the phase, for example, in the case

of the soliton in Fig. 2(d).

Finally, we consider the case of a repulsive intraspecies interaction and an attractive interspecies interaction, employing the parameters $c_0 = 0.5, c_2 = -0.5$ and $d = 2$. For an SO-coupling strength $\gamma = 0$ and dipolar interaction $d = 0$, in this case there is no binary soliton, confirming net repulsion in the model. For both $\gamma = 0.1$ and 1, there is only a single state – the bright-bright soliton illustrated in Figs. 3(a) and (b), respectively. The dark-bright soliton and the phase-separated bright-bright soliton are not possible here, as the imaginary-time propagation converges to a magnetization $|\mathcal{M}|$ unity or no atoms in the dark component. There is also no soliton in this case with spatially periodic stripe in density. The strong interspecies contact attraction and the dipolar attraction squeeze the solitons to the central region and do not permit the formation of density modulation over a larger region of space. In this case the component and total densities of the solitons in Figs. 3(a) and 3(b) for $\gamma_1 = 0.1$ and $\gamma_2 = 1$, respectively, are identical and the two energies $E_1 = -0.041$ and $E_2 = -0.536$ satisfy the relation (48).

B. Quasi-1D SO-coupled spin-one self-repulsive dipolar BEC soliton

We now consider the scenario of soliton formation in a quasi-1D self-repulsive SO-coupled dipolar spin-one BEC. In this case there are two contact interaction parameters c_0 and c_2 . First, we consider an anti-ferromagnetic BEC originating from a positive $c_2 > 0$ [66]. To study the case of an anti-ferromagnetic BEC, we consider the parameters $c_0 = c_2 = 0.5, d = 2$. In this case also, for $d = \gamma = 0$, there is no soliton formation. We find three types of solitons in this case: partially phase-separated bright-bright-bright, dark-bright-dark, and bright-dark-bright solitons as displayed in Figs. 4(a)-(c), in increasing order of energy. The solitons in Figs. 4(b)-(c) are excited metastable states. The partially phase-separated bright-bright-bright soliton can only be obtained with the SO coupling $\gamma\Sigma_x p_x$, all other solitons in this case can be obtained with both types of SO coupling $\gamma\Sigma_x p_x$ and $\gamma\Sigma_y p_x$. For a large $\gamma = 1$, there are only following two quasi-degenerate solitons with a spatially-periodic modulation in density: dark-bright-dark and bright-dark-bright solitons illustrated in Figs. 4(d)-(e), respectively. In Fig. 4(f) we plot the phase of the wave function of the three components of the dark-bright-dark soliton presented in Fig. 4(a). As expected [23] the phase of the dark components shows a jump of π at the origin while that of the bright component is zero.

Next we study the formation of quasi-1D solitons in a ferromagnetic SO-coupled spin-one dipolar BEC employing the parameters $c_0 = 0.5, c_2 = -0.1, d = 2$. In this case also, for $d = \gamma = 0$, there is no soliton formation. For $\gamma = 0.1$, one can have only two types of distinct solitons,

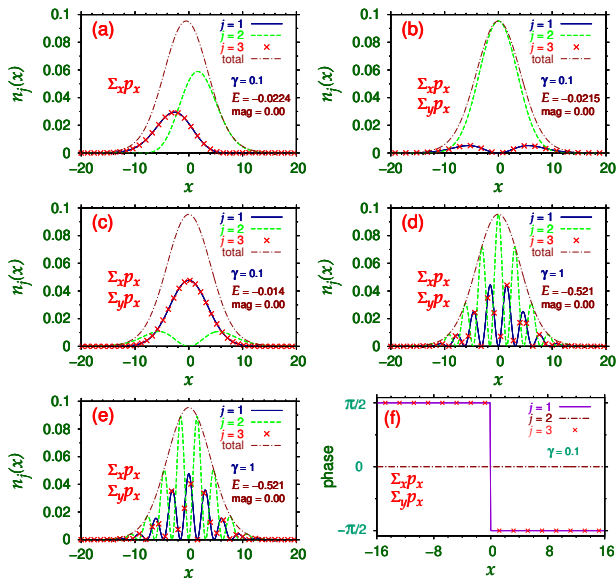


FIG. 4: Density of components $j = 1, 2, 3$ and total density of a quasi-1D SO-coupled spin-one dipolar (a) dark-bright-dark, (b) partially phase-separated bright-bright-bright and (c) bright-dark-bright solitons for SO-coupling strength $\gamma = 0.1$ for an anti-ferromagnetic spin-one BEC. The plots (d)-(e) display a dark-bright-dark and a bright-dark-bright soliton, both with a spatially-periodic modulation in density, respectively for $\gamma = 1$. The plot (f) depicts the phase of the component wave functions of the soliton of plot (a). The parameters are $c_0 = 0.5, c_2 = 0.5, d = 2$.

as illustrated in Fig. 5, (a) a bright-bright-bright soliton and (b) a phase-separated bright-bright-bright soliton. This phase-separated bright-bright-bright soliton was obtained by introducing a relative phase of $-\pi$ between components $j = 1$ and 3 in the initial state to generate a repulsion between these two components. Because of this additional repulsion, the phase-separated bright-bright-bright soliton of Fig. 5(b) appears as an excited metastable state. The phase-separated soliton of Fig. 5(b) is distinct from the partially phase-separated bright-bright-bright soliton in the anti-ferromagnetic case, viz. Fig. 4(a). For $\gamma = 0.1$, the quasi-1D solitons in the ferromagnetic BEC are completely distinct from the quasi-1D solitons in the anti-ferromagnetic case, viz. Fig. 4(a)-(c), with no dark soliton component in the ferromagnetic case. For a large SO-coupling strength ($\gamma = 1$), the only possible soliton is of the bright-bright-bright type as shown in Figs. 5(c). In this case the component and total densities of the solitons in Figs. 5(a) and 5(e) for $\gamma_1 = 0.1$ and $\gamma_2 = 1$, respectively, are identical and the two energies $E_1 = -0.026$ and $E_2 = -0.521$ satisfy the relation (48).

C. Dynamical stability of the solitons

The solitons presented in Figs. 1-5, for the same set of

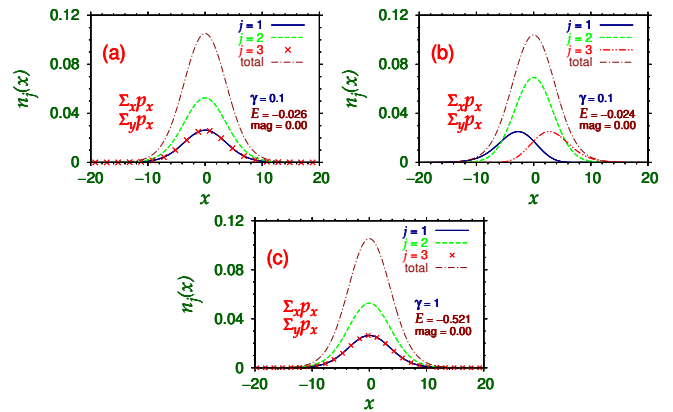


FIG. 5: Density of components $j = 1, 2, 3$ and total density of a quasi-1D SO-coupled spin-one dipolar (a) bright-bright-bright, (b) a phase-separated bright-bright-bright solitons for SO-coupling strength $\gamma = 0.1$ for a ferromagnetic spin-one BEC. The plot (c) displays a bright-bright-bright soliton for $\gamma = 1$. The parameters are $c_0 = 0.5, c_2 = -0.1, d = 2$.

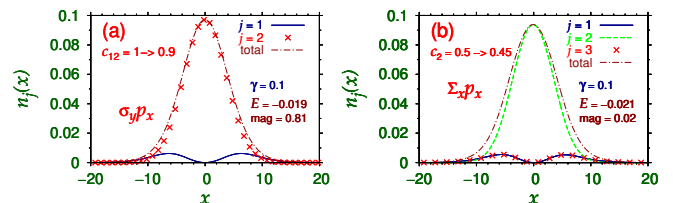


FIG. 6: (a) Density of components $j = 1, 2$ and total density of the quasi-1D SO-coupled pseudo spin-half dark-bright dipolar soliton of Fig. 1(a) after real-time propagation for 250 units of time, while the contact interaction parameter c_2 was changed from 1 to 0.9 at the start of the dynamics. (b) Density of components $j = 1, 2, 3$ and total density of the quasi-1D SO-coupled spin-one dark-bright-dark dipolar soliton of Fig. 4(a) after real-time propagation for 250 units of time, while the contact interaction parameter c_2 was changed from 0.5 to 0.45 at the start of the dynamics.

parameters, are often quasi-degenerate, viz. Figs. 1(a)-(c); sometimes they are excited states, viz. Figs. 2(b), 2(e), 4(b)-(c) and 5(b). This could make their experimental observation difficult, as these states could transform to their degenerate counterpart or else they can decay to the ground state. Imaginary-time propagation method usually finds the lowest-energy state with a definite symmetry property. For example, in a quasi-1D single-component harmonically trapped BEC it can find the lowest-energy parity-symmetric state (ground state) as well as the lowest-energy parity-antisymmetric state (the first excited state), which is a dark soliton with a zero density at the middle. The dark soliton state, although obtained by imaginary-time propagation approach, is dynamically unstable, as it eventually decays to the parity-symmetric ground state. This makes the experimental observation of dark solitons very difficult. The solitons can be observed if they are dynamically sta-

ble.

To study the dynamical stability of the present SO-coupled quasi-1D pseudo spin-half and spin-one dipolar solitons, we pay special attention to the soliton complexes with a dark soliton component, because dark solitons in a single-component BEC are unstable in general [21, 24–26]. We find that all the solitons studied in this paper are dynamically stable. We present results of stability of the pseudo spin-half dark-bright soliton depicted in Fig. 1(a) and the spin-one dark-bright-dark soliton illustrated in Fig. 4(a), both with a dark soliton component. First, we consider the converged imaginary-time wave function of the pseudo spin-half SO-coupled dipolar dark-bright soliton for $\gamma = 0.1$, viz. Fig. 1(a), and perform real-time simulation after changing the nonlinearity c_2 from 1 to 0.9 at time $t = 0$ using the imaginary-time wave function as the initial state. The resultant real-time density at time $t = 250$ units of time is displayed in Fig. 6(a), which compares well with the imaginary-time density of Fig. 1(a), demonstrating the dynamical stability of the soliton. Although, the final energy $E = -0.19$ after real-time propagation in Fig. 6(a) is quite close to the imaginary-time energy $E = -0.20$, the final magnetization $\mathcal{M} = -0.81$ after real-time propagation is a bit different from the imaginary-time magnetization $\mathcal{M} = -0.69$. This difference in magnetization is due to a decrease in interspecies repulsion in real-time propagation.

To establish the dynamical stability of the spin-one dark-bright-dark SO-coupled dipolar soliton of Fig. 4(a), we use the converged imaginary-time wave function of this soliton as the initial state in a real-time propagation after changing the nonlinearity parameter c_2 from 0.5 to 0.45 at time $t = 0$. The resultant real-time density at time $t = 250$ units of time is displayed in Fig. 6(b), in good agreement of the imaginary-time density of Fig. 4(a), which demonstrates the dynamical stability. The final energy $E = -0.21$ after real-time propagation in Fig. 6(b) is quite close to the imaginary-time energy $E = -0.22$.

V. SUMMARY AND DISCUSSION

To search for a quasi-1D soliton in a uniform pseudo spin-half and spin-one SO-coupled dipolar, self-repulsive BEC, using the numerical solution of a mean-field model, we identify different types of solitons. In the absence of an SO coupling and a dipolar interaction, the net prevailing interaction in all the systems, considered in this paper, is repulsive and no solitons can be formed, which justifies the term self-repulsive. In the pseudo spin-half case, for repulsive intraspecies and interspecies contact interactions, for a small SO-coupling strength ($\gamma = 0.1$), there are dark-bright, and phase-separated and overlapping bright-bright solitons, viz. Figs. 1(a)-(c). For an attractive intraspecies and a repulsive interspecies contact interaction, for a small γ , we have only dark-bright

and bright-bright solitons, viz. Figs. 2(a)-(b). For a repulsive intraspecies and an attractive interspecies contact interaction, for all γ ($= 0.1$, and 1), only the overlapping bright-bright soliton of Fig. 1(c) is possible, viz. Fig. 3(a)-(b). For a large SO-coupling strength ($\gamma = 1$), for repulsive interspecies interaction and both attractive and repulsive intraspecies interactions, the scenario of soliton formation is the same and we can have (A) a dark-bright soliton, (B) a phase-separated bright-bright soliton, and (C) an overlapping bright-bright soliton, viz. Figs. 1(d)-(f) and Figs. 2(c)-(e). The first two of these solitons, e.g. (A) and (B), are quasi-degenerate and also have a spatially-periodic modulation in density. The overlapping bright-bright soliton of Fig. 1(f) is also degenerate with the other two solutions, whereas that of Fig. 2(e) is an excited metastable state.

In the spin-one anti-ferromagnetic case ($c_2 > 0$), for a weak SO coupling ($\gamma = 0.1$), there are three different types of solitons: a partially overlapping bright-bright-bright soliton, viz. Fig. 4(a), a dark-bright-dark soliton, viz. Fig. 4(b), and a bright-dark-bright soliton, viz. Fig. 4(c). In the ferromagnetic case, for $c_2 < 0$, $\gamma = 0.1$, we have completely different types of solitons: a bright-bright-bright soliton, viz. Fig. 5(a), and a phase-separated bright-bright-bright soliton, viz. Fig. 5(b). For a large $\gamma = 1$, in the anti-ferromagnetic case we have only a bright-dark-bright and a dark-bright-dark quasi-degenerate solitons with a spatially-periodic stripe in density as shown in Figs. 4(d)-(e). In the ferromagnetic case ($c_2 < 0$), for $\gamma = 1$, we only have a bright-bright-bright soliton, viz. 5(c).

The spatially-periodic modulation in density of these solitons [39, 68, 69, 71] is a manifestation of supersolid formation [72–75] in these systems. This supersolid formation was observed experimentally in a pseudo spin-half SO-coupled BEC of ^{23}Na atoms [68]. Although, a spatially-periodic modulation in density with a period of π/γ is clearly seen in the component densities in some cases, there is no such modulation in the total density, consistent with the analytic consideration in Secs. III A and III B.

The dark soliton in a single-component BEC or in nonlinear optics, being an excited state, is dynamically unstable. All solitons presented in this paper are dynamically stable, specially those with a dark soliton component. We demonstrated this for the pseudo spin-half dark-bright soliton of Fig. 1(a) and the spin-one bright-dark-bright soliton of Fig. 4(a) by real-time propagation over a long time interval after introducing a perturbation at the start of the dynamics, viz. Fig. 6.

Some of the solitons, viz. Figs. 2(b), 2(e), 4(b)-(c), and 5(b), presented in this paper are excited metastable states trapped in a local minimum of energy. Their existence, stability, and eventual decay are governed by an interplay between energetic (thermodynamic) considerations and the evolution of perturbations (dynamical stability). The imaginary-time propagation procedure has been adapted successfully for these metastable states,

starting with a trial wave function with a definite symmetry property. In addition, these solitons are dynamically stable, as verified by the real-time propagation procedure. The stability of these metastable states in both real- and imaginary-time procedures generally may assure the thermodynamic stability of these states, but this is not guaranteed. Being excited states, they could be thermodynamically unstable and suffer energetic decay to the ground state, with a global minimum of energy, and phonons. A full analysis of the thermodynamic stability of these states is beyond the scope of this paper.

We believe that the present study could motivate experiments in the search of the novel solitons in an SO-coupled pseudo spin-half and spin-one dipolar spinor BEC. The present solitons are dynamically robust and deserve further theoretical and experimental investigations.

ACKNOWLEDGMENT

The author acknowledges support by the Conselho Nacional de Desenvolvimento Científico e Tecnológico (Brazil) grant 303885/2024-6.

DATA AVAILABILITY

The data that support the findings of this article are not publicly available upon publication because it is not technically feasible and/or the cost of preparing, depositing, and hosting the data would be prohibitive within the terms of this research project. The data are available from the authors upon reasonable request.

-
- [1] O. Bang, W. Krolikowski, J. Wyller, and J. J. Rasmussen, *Phys. Rev. E* **66**, 046619 (2002).
- [2] Y. S. Kivshar and B. A. Malomed, *Rev. Mod. Phys.* **61**, 763 (1989).
- [3] F. K. Abdullaev, A. Gammal, A. M. Kamchatnov, and L. Tomio, *Int. J. Mod. Phys. B* **19**, 3415 (2005).
- [4] K. E. Strecker, G. B. Partridge, A. G. Truscott, and R. G. Hulet, *Nature (London)* **417**, 150 (2002).
- [5] L. Khaykovich, F. Schreck, G. Ferrari, T. Bourdel, J. Cubizolles, L. D. Carr, Y. Castin, and C. Salomon, *Science* **256**, 1290 (2002).
- [6] S. L. Cornish, S. T. Thompson, and C. E. Wieman, *Phys. Rev. Lett.* **96**, 170401 (2006).
- [7] S. Inouye, M. R. Andrews, J. Stenger, H.-J. Miesner, D. M. Stamper-Kurn, and W. Ketterle, *Nature (London)* **392**, 151 (1998).
- [8] V. M. Pérez-García, H. Michinel, and H. Herrero, *Phys. Rev. A* **57**, 3837 (1998).
- [9] E. P. Gross, *Nuovo Cim.* **20**, 454 (1961).
- [10] L.P. Pitaevskii, *Zurn. Eksp. Teor. Fiz.* **40**, 646 (1961)[English Transla.: *Sov. Phys. JETP.* **13**, 451 (1961)].
- [11] L. D. Carr, J. N. Kutz, and W. P. Reinhardt, *Phys. Rev. E* **63**, 066604 (2001).
- [12] O. L. Berman, R. Y. Kezerashvili, G. V. Kolmakov, and L. M. Pomirchi, *Phys. Rev. E* **91**, 062901 (2015).
- [13] L.-C. Zhao, *Phys. Rev. E* **97**, 062201 (2018).
- [14] N.-S. Wan, Y.-E. Li, and J.-K. Xue, *Phys. Rev. E* **99**, 062220 (2019).
- [15] P. Fang and J. Lin, *Phys. Rev. E* **109**, 064219 (2024).
- [16] M. Salerno and B. B. Baizakov, *Phys. Rev. E* **98**, 062220 (2018).
- [17] Y.-H. Qin, L.-C. Zhao, and L. Ling, *Phys. Rev. E* **100**, 022212 (2019).
- [18] D. N. Christodoulides, *Phys. Lett. A* **132**, 451 (1988).
- [19] D. Krökel, N. J. Halas, G. Giuliani, and D. Grischkowsky, *Phys. Rev. Lett.* **60**, 29 (1988).
- [20] R. Kashyap and K. J. Blow, *Electronics Lett.* **24**, 47 (1988).
- [21] S. Burger, K. Bongs, S. Dettmer, W. Ertmer, K. Sengstock, A. Sanpera, G. V. Shlyapnikov, and M. Lewenstein, *Phys. Rev. Lett.* **83**, 5198 (1999).
- [22] J. Denschlag, J. E. Simsarian, D. L. Feder, C. W. Clark, L. A. Collins, J. Cubizolles, L. Deng, E. W. Hagley, K. Helmerson, W. P. Reinhardt, S. L. Rolston, B. I. Schneider, and W. D. Phillips, *Science* **287**, 97 (2000).
- [23] D. J. Frantzeskakis, *J. Phys. A: Math. Theor.* **43** 213001 (2010).
- [24] B. P. Anderson, P. C. Haljan, C. A. Regal, D. L. Feder, L. A. Collins, C. W. Clark, and E. A. Cornell, *Phys. Rev. Lett.* **86**, 2926 (2001).
- [25] G. Lombardi, W. Van Alphen, S. N. Klimin, and J. Tempere, *Phys. Rev. A* **96**, 033609 (2017).
- [26] Y. S. Kivshar and W. Królikowski, *Opt. Lett.* **20**, 1527 (1995).
- [27] F. Dalfovo, S. Giorgini, L. P. Pitaevskii, and S. Stringari, *Rev. Mod. Phys.* **71**, 463 (1999).
- [28] J. Stenger, S. Inouye, D. M. Stamper-Kurn, H.-J. Miesner, A. P. Chikkatur, and W. Ketterle, *Nature (London)* **396**, 345 (1998).
- [29] V. Galitski and I. B. Spielman, *Nature (London)* **494**, 49 (2013).
- [30] D. Campbell, R. Price, A. Putra, A. Valdés-Curiel, D. Trypogeorgos, and I. B. Spielman, *Nat. Commun.* **7**, 10897 (2016).
- [31] Y.-J. Lin, R. L. Compton, K. Jiménez-García, W. D. Phillips, J. V. Porto, and I. B. Spielman, *Nature Phys.* **7**, 531 (2011).
- [32] J. Dalibard, F. Gerbier, G. Juzeliunas, and P. Öhberg, *Rev. Mod. Phys.* **83**, 1523 (2011).
- [33] Y.-J. Lin, K. Jiménez-García, and I. B. Spielman, *Nature (London)* **471**, 83 (2011).
- [34] J. Li, W. Huang, B. Shteynas, S. Burchesky, F. Ç. Top, E. Su, J. Lee, A. O. Jamison, and W. Ketterle, *Phys. Rev. Lett.* **117**, 185301 (2016).
- [35] T. Mizushima, K. Machida, and T. Kita, *Phys. Rev. Lett.* **89**, 030401 (2002).
- [36] T. Mizushima, K. Machida, and T. Kita, *Phys. Rev. A* **66**, 053610 (2002).
- [37] V. Achilleos, D. J. Frantzeskakis, P. G. Kevrekidis, and D. E. Pelinovsky, *Phys. Rev. Lett.* **110**, 264101 (2013).
- [38] S. Gautam and S. K. Adhikari, *Laser Phys. Lett.* **12**, 045501 (2015).

- [39] Y. Li, G. I. Martone, L. P. Pitaevskii, and S. Stringari, *Phys. Rev. Lett.* 110, 235302 (2013).
- [40] T. Lahaye, C. Menotti, L. Santos, M. Lewenstein, and T. Pfau, *Rep. Prog. Phys.* 72, 126401 (2009).
- [41] T. Lahaye, T. Koch, B. Fröhlich, M. Fattori, J. Metz, A. Griesmaier, S. Giovanazzi, and T. Pfau, *Nature (London)* 448, 672 (2007).
- [42] T. Koch, T. Lahaye, J. Metz, B. Fröhlich, A. Griesmaier, and T. Pfau, *Nature Phys.* 4, 218 (2008).
- [43] L. Chomaz, S. Baier, D. Petter, M. J. Mark, F. Wächtler, L. Santos, and F. Ferlaino, *Phys. Rev. X* 6, 041039 (2016).
- [44] K. Aikawa, A. Frisch, M. Mark, S. Baier, A. Rietzler, R. Grimm, and F. Ferlaino, *Phys. Rev. Lett.* 108, 210401 (2012).
- [45] M. Lu, S. H. Youn, and B. L. Lev, *Phys. Rev. Lett.* 104, 063001 (2010).
- [46] S. H. Youn, M. W. Lu, U. Ray, and B. L. Lev, *Phys. Rev. A* 82, 043425 (2010).
- [47] M. Kato, X.-F. Zhang, D. Sasaki, and H. Saito, *Phys. Rev. A* 94, 043633 (2016).
- [48] Y. Deng, J. Cheng, H. Jing, C.-P. Sun, and S. Yi, *Phys. Rev. Lett.* 108, 125301 (2012).
- [49] S.-C. Ji, L. Zhang, X.-T. Xu, Z. Wu, Y. Deng, S. Chen, and J.-W. Pan, *Phys. Rev. Lett.* 114, 105301 (2015)
- [50] R. M. Wilson, B. M. Anderson, and C. W. Clark, *Phys. Rev. Lett.* 111, 185303 (2013).
- [51] S. Gopalakrishnan, I. Martin, and E. A. Demler, *Phys. Rev. Lett.* 111, 185304 (2013).
- [52] E. Chiquillo, *Phys. Rev. A* 97, 013614 (2018).
- [53] C. Huang, Y. Ye, S. Liu, H. He, W. Pang, B. A. Malomed, and Y. Li, *Phys. Rev. A* 97, 013636 (2018).
- [54] X. Li, Q. Wang, H. Wang, C. Shi, M. Jardine, and L. Wen, *J. Phys. B* 52, 155302 (2019).
- [55] H. Yang, Q. Wang, and L. Wen, *J. Phys. Soc. Japan* 88, 064001 (2019).
- [56] V. I. Yukalov and E. P. Yukalova, *Laser Phys.* 26, 045501 (2016).
- [57] V. I. Yukalov, *Laser Phys.* 28, 053001 (2018).
- [58] L. Salasnich and B. A. Malomed, *Phys. Rev. A* 74, 053610 (2006).
- [59] V. Achilleos, D. J. Frantzeskakis, P. G. Kevrekidis, and D. E. Pelinovsky, *Phys. Rev. Lett.* 110, 264101 (2013).
- [60] Y. Xu, Y. Zhang, and B. Wu, *Phys. Rev. A* 87, 013614 (2013).
- [61] H. Sakaguchi, B. Li, and B. A. Malomed, *Phys. Rev. E* 89, 032920 (2014).
- [62] H. Sakaguchi and B. A. Malomed, *Phys. Rev. E* 90, 062922 (2014).
- [63] Y.-C. Zhang, Z.-W. Zhou, B. A. Malomed, and H. Pu, *Phys. Rev. Lett.* 115, 253902 (2015).
- [64] V. M. Perez-García and J. B. Beitia, *Phys. Rev. A* 72, 033620 (2005).
- [65] S. K. Adhikari, *Phys. Lett. A* 346, 179 (2005).
- [66] Y. Kawaguchi and M. Ueda, *Phys. Rep.* 520, 253 (2012).
- [67] J. Li, W. Huang, B. Shteynas, S. Burchesky, F. Ç. Top, E. Su, J. Lee, A. O. Jamison, and W. Ketterle, *Phys. Rev. Lett.* 117, 185301 (2016).
- [68] J.-R. Li, J. Lee, W. Huang, S. Burchesky, B. Shteynas, F. Ç. Top, A. O. Jamison, and W. Ketterle, *Nature (London)* 543, 91 (2017).
- [69] T. Ozawa and G. Baym, *Phys. Rev. Lett.* 109, 025301 (2012).
- [70] T. Ozawa and G. Baym, *Phys. Rev. Lett.* 110, 085304 (2013)
- [71] A. Putra, F. Salces-Carcoba, Y. Yue, S. Sugawa, and I. B. Spielman, *Phys. Rev. Lett.* 124, 053605 (2020).
- [72] E.P. Gross, *Phys. Rev.* 106, 161 (1957).
- [73] A. F. Andreev and I. M. Lifshitz, *Zurn. Eksp. Teor. Fiz.* 56, 2057 (1969) [English Transla.: *Sov. Phys. JETP* 29, 1107 (1969)].
- [74] A. J. Leggett, *Phys. Rev. Lett.* 25, 1543 (1970).
- [75] G. V. Chester, *Phys. Rev. A* 2, 256 (1970).
- [76] V. I. Yukalov, *Phys.* 2, 49 (2020).
- [77] D. Mihalache, *Rom. Rep. Phys.* 73, 403 (2021).
- [78] G. Dresselhaus, *Phys. Rev.* 100, 580 (1955).
- [79] Y. A. Bychkov and E. I. Rashba, *J. Phys. C: Solid State Phys.* 17, 6039 (1984).
- [80] E. I. Rashba, *Fiz. Tverd. Tela* 2, 1224 (1960) [English Transla.: *Sov. Phys. Solid State* 2, 1109 (1960).]
- [81] W. Bao and Y. Cai, *Commun. Comput. Phys.* 24, 899 (2018).
- [82] L. Salasnich, A. Parola, and L. Reatto, *Phys. Rev. A* 65, 043614 (2002)
- [83] R. Kishor Kumar, L. E. Young-S., D. Vudragović, A. Balaž, P. Muruganandam, and S. K. Adhikari, *Comput. Phys. Commun.* 195, 117 (2015).
- [84] T. Ohmi and K. Machida, *J. Phys. Soc. Japan* 67, 1822 (1998).
- [85] T. L. Ho, *Phys. Rev. Lett.* 81, 742 (1998).
- [86] E. G. M. Van kempen, S. J. J. M. F. Kokkelmans, D. J. Heinzen, and B. J. Verhaar, *Phys. Rev. Lett.* 88, 093201 (2002);
- [87] M.-S. Chang, Q. Qin, W. Zhang, L. You, and M. S. Chapman, *Nature Phys.* 1, 111 (2005).
- [88] A. Widera, F. Gerbier, S. Fölling, T. Gericke, O. Mandel, and I. Bloch, *New J. Phys.* 8, 152 (2006).
- [89] A. T. Black, E. Gomez, L. D. Turner, S. Jung, and P. D. Lett, *Phys. Rev. Lett.* 99, 070403 (2007).
- [90] P. Muruganandam and S. K. Adhikari, *Comput. Phys. Commun.* 180, 1888 (2009)
- [91] I. Ferrier-Barbut, H. Kadau, M. Schmitt, M. Wenzel, and T. Pfau, *Phys. Rev. Lett.* 116, 215301 (2016).
- [92] V. Lončar, L. E. Young-S., S. Škrbić, P. Muruganandam, S. K. Adhikari, and A. Balaž, *Comput. Phys. Commun.* 209, 190 (2016).
- [93] R. Ravisankar, D. Vudragović, P. Muruganandam, A. Balaž, and S. K. Adhikari, *Comput. Phys. Commun.* 259, 107657 (2021)